



Since January 2020 Elsevier has created a COVID-19 resource centre with free information in English and Mandarin on the novel coronavirus COVID-19. The COVID-19 resource centre is hosted on Elsevier Connect, the company's public news and information website.

Elsevier hereby grants permission to make all its COVID-19-related research that is available on the COVID-19 resource centre - including this research content - immediately available in PubMed Central and other publicly funded repositories, such as the WHO COVID database with rights for unrestricted research re-use and analyses in any form or by any means with acknowledgement of the original source. These permissions are granted for free by Elsevier for as long as the COVID-19 resource centre remains active.

TWO NEUROTROPIC VIRUSES, HERPES SIMPLEX VIRUS TYPE 1 AND MOUSE HEPATITIS VIRUS, SPREAD ALONG DIFFERENT NEURAL PATHWAYS FROM THE MAIN OLFATORY BULB

E. M. BARNETT,* M. D. CASSELL*† and S. PERLMAN*‡§

*Neuroscience Program, †Department of Anatomy, ‡Departments of Pediatrics and Microbiology, University of Iowa College of Medicine, Iowa City, IA 52242, U.S.A.

Abstract—Several neurotropic viruses enter the brain after peripheral inoculation and spread transneuronally along pathways known to be connected to the initial site of entry. In this study, the pathways utilized by two such viruses, herpes simplex virus type 1 and mouse hepatitis virus strain JHM, were compared using *in situ* hybridization following inoculation into either the nasal cavity or the main olfactory bulb of the mouse. The results indicate that both viruses spread to infect a unique and only partially overlapping set of connections of the main olfactory bulb. Both quantitative and qualitative differences were observed in the patterns of infection of known primary and secondary main olfactory bulb connections. Using immunohistochemistry for tyrosine hydroxylase combined with *in situ* hybridization, it was shown that only herpes simplex virus infected noradrenergic neurons in the locus coeruleus. In contrast, both viruses infected dopaminergic neurons in the ventral tegmental area, although mouse hepatitis virus produced a more widespread infection in the A10 group, as well as infecting A8 and A9.

The results suggest that differential virus uptake in specific neurotransmitter systems contributes to the pattern of viral spread, although other factors, such as differences in access to particular synapses on infected cells and differences in the distribution of the cellular receptor for the two viruses, are also likely to be important. The data show that neural tracing with different viruses may define unique neural pathways from a site of inoculation. The data also demonstrate that two viruses can enter the brain via the olfactory system and localize to different structures, suggesting that neurological diseases involving disparate regions of the brain could be caused by different viruses, even if entry occurred at a common site.

A number of viruses have been shown to spread transneuronally into and throughout the rodent CNS following intranasal inoculation, including herpes simplex virus type 1 (HSV-1),⁷⁵ vesicular stomatitis virus,⁴³ Borna disease virus,⁵¹ mouse hepatitis virus (MHV),^{40,55} pseudorabies virus³⁴ and rabies virus.³⁸ Virus spread through the olfactory system is of particular importance since the olfactory receptor neuroepithelial cells are the only neurons with direct exposure to the environment. As such, the olfactory system is a likely route of entry for viruses and toxins into the CNS and the distribution of lesions in some human diseases, such as Alzheimer's disease, is consistent with spread of an environmental agent into the CNS via the olfactory system.

MHV belongs to the coronavirus family of enveloped, positive-stranded RNA viruses. Although some coronaviruses infect humans, causing respiratory in-

fections such as the common cold, coronavirus pathogenesis research has focused primarily on animal infections. Rodent infections with neurotropic strains of MHV have been studied as models for acute and chronic virus-related neurological disease.^{9,39,80} Strain JHM (MHV-JHM) is highly neurotropic and causes a fatal acute encephalitis following intranasal inoculation of suckling and adult C57Bl/6 mice.⁵³ Mice passively immunized against the virus or infected with an attenuated strain do not develop an acute encephalitis, but instead often manifest a chronic demyelinating disease characterized by hind-limb paralysis.^{6,10,18,26,53} This virus-induced demyelination serves as a model for multiple sclerosis.

Evidence from several studies indicates that MHV enters the CNS via the olfactory nerve following intranasal inoculation and spreads to many of the primary and secondary connections of the main olfactory bulb (MOB).^{3,21,40,54,55} Both chemical deafferentation and surgical removal of the MOB prior to intranasal inoculation prevent CNS entry and show that virus entry via the trigeminal nerve is insignificant.^{2,56} The structures infected by MHV-JHM and the temporal sequence of their infection strongly suggests that this virus, like many other neurotropic viruses, spreads transneuronally into and throughout the CNS.

§To whom correspondence should be addressed.

Abbreviations: HSV-1, herpes simplex virus, type 1; LC, locus coeruleus; MHV-JHM, mouse hepatitis virus, strain JHM; MOB, main olfactory bulb; PFU, plaque forming unit; p.i. post-inoculation; TH, tyrosine hydroxylase; TH+, tyrosine hydroxylase immunoreactive; TH-, tyrosine hydroxylase immunonegative; VTA, ventral tegmental area; WGA-HRP, wheatgerm agglutinin-horseradish peroxidase.

HSV-1 is a human pathogen which usually causes recurrent, localized vesicular lesions, but is also an important cause of sporadic cases of severe encephalitis. HSV-1 causes encephalitis in mice and rats following intranasal inoculation^{29,47} and, unlike MHV-JHM, can enter the rodent CNS from peripheral inoculation sites such as the tongue,⁷⁴ the eye³⁵ and the tooth pulp (Barnett E. M., Jacobsen G. and Perlman S., unpublished data). As is the case with MHV-JHM, the pattern of the resulting infection is suggestive of transneuronal movement of virus and, as such, HSV-1 has proved useful for tracing neural circuits.^{5,28,47}

Our initial studies with MHV-JHM suggested that after intranasal inoculation the virus spread along different pathways from the MOB as compared to previous studies with HSV-1. For example, several workers^{47,75} reported HSV-1 infection of the locus coeruleus (LC) in rats and mice following MOB infection, whereas we could not detect MHV-JHM in this structure. Based on these preliminary results, we determined the extent to which these two neurotropic viruses infected different CNS structures after infection of the MOB. Although studies have been performed describing the pattern of virus spread for wild-type and attenuated strains of several neurotropic viruses,^{8,36,44} this is the first to compare the transneuronal spread of two different viruses using exactly the same experimental design. The possible differential spread of viruses throughout the brain has important implications for the use of viruses such as HSV-1 as neuroanatomical tracers, as it has been generally assumed that such viruses spread non-specifically throughout the CNS along all the available pathways from an infected structure. Such differential localization would also suggest that different viruses could cause different neurological diseases, depending on precisely which connections of the olfactory nerve were infected.

EXPERIMENTAL PROCEDURES

Animals

Twelve male suckling (10-day-old) and 24 male young adult (six-week-old) C57Bl/6 mice purchased from Sasco Laboratories (Omaha, NE) were used in these studies. For surgeries, mice were anesthetized by intraperitoneal injections of a sodium pentobarbital solution (52.5 mg/kg).⁶⁴ All surgical procedures were approved by the Institutional Animal Care and Use Committee at the University of Iowa.

Virus

MHV-JHM was grown on BALB/c 17Cl-1 cells and HSV-1 on RK13 cells. The two viruses were titrated and maintained frozen at -70°C in tissue culture media. Strain 17 (kindly provided by Dr Moira Brown), a highly neurovirulent strain of HSV-1,¹³ caused encephalitis after intranasal inoculation in suckling C57Bl/6 mice and was used in all studies. Consistent with other reports, adult C57Bl/6 mice were resistant to even this strain of HSV-1 after intranasal inoculation,²⁹ but preliminary experiments indicated that these mice could be infected with HSV-1 by intrabulbar inoculation.

Inoculations

We compared the distributions of HSV-1 and MHV-JHM in the brains of suckling C57Bl/6 mice following intranasal inoculation and young adult C57Bl/6 mice following intrabulbar inoculations. The use of both intranasal and intrabulbar inoculations served three purposes. First, intrabulbar inoculation eliminated trigeminal entry of HSV-1 so that the pattern of infection would reflect viral spread from the MOB. Second the use of intranasal inoculations ensured that differences in the movement of the viruses into and throughout the internal circuitry of the MOB would become apparent. Third, inoculation of HSV-1 into the MOB made possible the use of older C57Bl/6 mice in which the infections spread more slowly, allowing for the examination of several time points during the course of the infection.

Ten-day-old mice received intranasal inoculations of approximately 10^3 plaque forming units (PFU) of MHV-JHM or 10^6 PFU of HSV-1 strain 17 in a volume of $10\ \mu\text{l}$. Six-week-old mice underwent direct bulb inoculations with one of the two viruses as follows. Following exposure of the skull over the olfactory bulbs, a small bone defect was produced over the left bulb using a dental drill. The dura was gently removed and 200 nl of MHV-JHM (10^3 PFU) or HSV-1 (10^4 PFU) was introduced into the center of the bulb by pressure injection using a glass micropipette (tip diameter $50\ \mu\text{m}$) attached to a $1\ \mu\text{l}$ Hamilton syringe. Co-inoculation of 100 nl of MHV-JHM and 100 nl of wheatgerm agglutinin-horseradish peroxidase (WGA-HRP; 1%) was performed in four mice to confirm the site of inoculation. Following inoculation the mice were observed over the next several days for signs of encephalitis such as irritability, ruffled fur, hunched backs and ataxia. Mice were killed over a period of days post-inoculation (p.i.), during which the appearance of the animals ranged from asymptomatic to nearly moribund. *In situ* hybridization was performed to determine the optimal times p.i. for neuroanatomical localization of viral nucleic acids. Four to six mice at each age, for both of the viruses, were inoculated and killed at the optimal time(s) p.i.: four days for all 10-day-old mice, three and four days for MHV-JHM-infected adult mice, and four and five days for HSV-1-infected adult mice. At earlier times p.i., virus had infected the MOB and only a few MOB connections. At later times, viral infection of the brain was so widespread as to make neuroanatomical localization of viral nucleic acid difficult.

As a control for viral spread via the cerebrospinal fluid, direct inoculation into the lateral ventricle of 200 nl of virus was performed on young adult C57Bl/6 mice with each virus. Stereotaxic coordinates for ventricular injections (AP -0.5 ; lateral 1.7 ; horizontal 2 mm) were taken from the stereotaxic mouse atlas of Slotnick and Leonard.⁶⁷ The MHV-JHM- and HSV-1-infected mice were killed at four and five days p.i., respectively, and *in situ* hybridization was performed.

In situ hybridization

An antisense ^{35}S -labeled RNA probe for MHV-JHM was synthesized and *in situ* hybridization performed as described previously.³⁴ Briefly, mice were deeply anesthetized and exsanguinated by transcardiac perfusion with 20 ml of phosphate-buffered saline and $35\ \mu\text{m}$ coronal brain sections were cut at $100\ \mu\text{m}$ intervals on a cryostat. Sections were collected on silane-treated slides, fixed, treated with proteinase K and acetylated. Approximately 10^6 c.p.m. of ^{35}S -labeled antisense RNA probe in hybridization solution was applied to each slide. After annealing overnight, slides were treated with RNase and washes of increasing stringency. Slides were then placed on film for several days at 4°C , followed by dipping in NTB-2 photographic emulsion (Kodak, Rochester, NY) for a two week exposure. After development and staining with Cresyl Violet, slides were examined by bright-field and dark-field light microscopy to localize viral nucleic acid in the brain. A plasmid construct contain-

ing the coding sequence for the VP5 gene of HSV-1 was obtained (kindly provided by Dr Ed Wagner) and RNA probe produced under the same protocol used for the production of MHV-JHM probe. *In situ* hybridization for HSV-1 was performed as for MHV-JHM with two modifications: before hybridization the slides were heated at 98°C for 3 min to denature viral DNA and hybridization took place overnight at 55°C rather than 45°C. Since HSV-1 is a DNA virus, the added denaturation step enabled the RNA probe to bind to both viral RNA and genomic viral DNA, producing a robust signal. The tetramethylbenzidine method of Mesulam⁴⁹ was used to visualize HRP in MOB sections from mice co-inoculated with MHV-JHM and WGA-HRP.

Combined immunohistochemistry and in situ hybridization

Six-week-old mice received intrabulbar inoculations with either virus, as described above. Three mice each were killed at 4.5 days p.i. for HSV-1 and four days p.i. for MHV-JHM. Two additional mice were killed at three days p.i. for MHV-JHM. Each mouse was anesthetized and killed by transcardiac perfusion fixation with 50 ml of periodate-lysine-paraformaldehyde fixative.⁴⁶ The brain was then removed and postfixed for 2 h in the same fixative. Cryostat sections (25 µm) were cut through the caudal forebrain and brainstem at 100 µm intervals and placed on silane-treated slides. The sections were incubated in phosphate-buffered saline for 15 min, 4% normal goat serum in 0.05% Triton X-100-phosphate-buffered saline for 1 hour, and rabbit anti-tyrosine hydroxylase (TH; Chemicon, Temecula, CA) overnight in 0.05% Triton X-100-phosphate-buffered saline at 4°C. The antigen-antibody complex was visualized using the Vector ABC method as specified by the manufacturer (Vector Labs, Burlingame, CA) with 3,3'-diaminobenzidine as the final substrate. RNasin (50 U/ml; Promega, Madison, WI) and heparin (5 mg/ml) were used to inhibit RNase activity during steps containing serum products.⁷⁹ All buffers and solutions used during the procedure were treated with diethylpyrocarbonate and autoclaved to eliminate RNase activity. Following immunohistochemistry for TH, *in situ* hybridization was performed as above to detect viral nucleic acid. Brain sections were examined for cells containing both TH immunoreactivity and silver grains.

RESULTS

In this study, HSV-1 and MHV-JHM infected a unique and partially overlapping set of structures following both intranasal and intrabulbar inoculation. The structures infected following intranasal inoculations in suckling mice and intrabulbar inoculations in young adult mice for each virus were almost identical. The main difference, as expected, was HSV-1 infection of the spinal tract and sensory root of the trigeminal nucleus following intranasal, but not intrabulbar inoculation. Although there is evidence for trigeminal innervation of the MOB,¹⁷ HSV-1 did not infect trigeminal nuclei following inoculation into the MOB. Given the high similarity of the results across the two types of inoculations, only the results for intrabulbar inoculations in young adult mice will be presented.

At the first time point examined (day 3 MHV-JHM, day 4 HSV-1) virus had already spread to the opposite hemisphere and most structures were infected bilaterally. Although virus spread was more extensive on the side of bulbar inoculation, the pattern of labeling was highly similar on both sides

by the second time point examined (day 4 MHV-JHM, day 5 HSV-1). Consistent with our previous experience with MHV-JHM, some structures were only infected in a subset of cases at a particular time p.i. These structures eventually became infected in all cases at later times p.i., however, suggesting that this variability reflected differences between mice in the temporal course of infection rather than in the pattern of spread.

Structures infected following intrabulbar inoculation (see Table 1)

Olfactory system. Both viruses regularly infected cells in the periglomerular, mitral and internal granular layers of the MOB. HSV-1 infected well-circumscribed regions of the internal granular layer, infecting large numbers of adjacent cells. In contrast, MHV-JHM infected more evenly distributed cells in this layer. Infection of the MOB did not differ significantly across the two types of inoculation for either virus. Examination of MOB sections from mice co-inoculated with WGA-HRP showed that the injection site was restricted to the bulb, but commonly involved all layers. Few HSV-1- or MHV-JHM-infected cells were seen in the two white matter layers, the external and internal plexiform layers. The accessory olfactory bulb was commonly infected by both viruses.

The anterior olfactory nucleus was infected by both viruses in all cases. MHV-JHM infected sparsely distributed cells in both the cellular and non-cellular layers of this nucleus (Fig. 1A). HSV-1 labeling was robust throughout the full extent of the cellular layer (Fig. 1B). Infection of the olfactory tubercle was seen in approximately one-half of the cases for either virus and was relatively light. The ventral tenia tecta was heavily infected by HSV-1 (Fig. 1D), but not at all by MHV-JHM (Fig. 1C). Although both viruses regularly infected the dorsal endopiriform nucleus, the ventral endopiriform nucleus was infected by MHV-JHM only. Labeling for MHV-JHM was commonly present over cells within the lateral olfactory tract by day 4 (Fig. 1A).

Cortex. HSV-1 infected a number of cortical areas, often producing extensive and specific laminar labeling. HSV-1 infection of the primary olfactory cortex was seen in every case. At day 4, virus was detected primarily in lamina 2b of the primary olfactory cortex, with scattered labeling in superficial lamina 3 (Fig. 2A, C). In more extensively infected brains, virus labeling was also seen in lamina 2a and throughout the full depth of lamina 3. Medial prefrontal cortex was commonly infected by day 4, with virus labeling in laminae 2, 3 and 5 of anterior cingulate cortex and laminae 2 and 3 of medial and lateral orbital cortices. By day 5, the infection had spread to involve almost every lamina of these cortical areas. Additional labeling was seen in laminae 2, 3 and 6 of medial agranular frontal cortex and 2, 5 and 6 of infralimbic cortex.

Table 1. Frequency of infection by MHV-JHM and HSV-1 following intrabulbar inoculation†

	MHV-JHM		HSV-1	
	Days p.i.		Days p.i.	
	3 (N = 4)	4 (N = 4)	4 (N = 4)	5 (N = 4)
Olfactory system				
Accessory olfactory bulb	—	****	*	***
Anterior olfactory nucleus	****	****	****	****
Ventral tenia tecta	—	—	***	****
Lateral olfactory tract	—	****	—	*
Olfactory tubercle	**	**	*	**
Dorsal endopiriform nucleus	****	****	***	****
Ventral endopiriform nucleus	—	****	—	—
Cortical				
Orbital	*	****	**	****
Anterior cingulate	*	****	***	****
Medial agranular frontal	—	—	**	***
Infralimbic	****	****	—	***
Primary olfactory	****	****	****	****
Agranular insular	*	****	***	****
Dysgranular insular	—	—	—	**
Granular insular	—	—	—	**
Parietal	—	—	—	**
Temporal	—	—	—	**
Perirhinal	****	****	**	****
Entorhinal	**	****	***	****
Basal forebrain				
Ventral pallidum	****	****	**	****
Medial septal nucleus	****	****	*	**
Horizontal nucleus of the diagonal band	****	****	**	****
Vertical nucleus of the diagonal band	****	****	—	—
Anterior commissure	****	****	—	**
Clastrum	*	**	—	**
Lateral septal nuclei	—	****	**	***
Triangular septal nucleus	*	****	—	—
Septofimbrial nucleus	***	****	—	—
Substantia innominata	****	****	*	*
Bed nuclei of stria terminalis	—	**	—	*
Lateral preoptic area	—	**	—	—
Amygdala				
Nucleus of lateral olfactory tract	*	—	**	***
Anterior	**	****	***	***
Anterior amygdaloid area	***	****	*	***
Basolateral	**	**	**	***
Basomedial	*	—	**	***
Central	—	—	—	***
Medial	**	****	**	***
Posterior lateral	**	**	***	****
Posterior medial	*	—	***	****
Diencephalon				
Paraventricular	—	**	***	***
Reuniens	—	*	**	***
Paratenial	—	**	**	***
Mediodorsal	—	**	—	*
Ventroposterior parvocellular	**	****	—	—
Lateral hypothalamic area	***	****	*	**
Anterior hypothalamic area: central	—	**	—	—
Posterior hypothalamic area	*	****	—	—
Zona incerta	—	**	—	—
Subthalamic nucleus	***	****	—	—
Lateral habenular nucleus	—	**	—	—
Stria medullaris	***	****	—	—
Hippocampal complex				
CA1	—	*	****	****
CA3	—	—	**	***
Dentate gyrus	—	—	—	***

continued

Table 1—Continued

	MHV-JHM		HSV-1	
	Days p.i.		Days p.i.	
	3 (N = 4)	4 (N = 4)	4 (N = 4)	5 (N = 4)
Subiculum	—	****	—	***
Anterior hippocampal continuation	—	*	*	**
Indusium griseum	—	****	—	—
Midbrain				
VTA	****	****	*	***
Substantia nigra: pars compacta	—	****	—	—
Caudal linear raphe	—	—	—	***
Dorsal raphe	***	***	***	***
Median raphe	*	*	—	**
Pedunculopontine tegmental	***	****	—	—
Medial parabrachial	**	****	—	—
LC	—	—	****	****
Pons and medulla				
Pontine reticular: oral	—	**	—	—
Pontine reticular: caudal	***	****	—	—
Gigantocellular	**	***	—	—
Raphe magnus	**	***	—	*
Raphe obscurus	**	****	—	*
A1 noradrenergic	—	—	—	**

†Each asterisk (*) denotes infection of the structure in an individual animal. Structures not infected by MHV-JHM or HSV-1 in at least two mice are not included.

Entorhinal cortex was also commonly infected by HSV-1 (Fig. 3C, D). At day 4, infection of laminae 2, 3 and 5 was already detectable in each case. At day 5, the infection had sometimes spread to every lamina of entorhinal cortex. Infection of perirhinal cortex was also detected in almost every case, beginning in lamina 5 at day 4 and spreading to involve laminae 2, 3, 5 and 6 at day 5. Agranular insular cortex was commonly infected in laminae 2, 5 and 6. Other cortical regions were labeled in more extensively infected brains, including laminae 2 and 6 of parietal cortex and lamina 2 of the granular insular, dysgranular insular and temporal cortices.

MHV-JHM also infected a number of cortical areas, although the labeling in specific cortical laminae was less extensive than with HSV-1. Primary olfactory cortex was infected by MHV-JHM in all cases. Whereas HSV-1 infection was concentrated primarily in lamina 2b, MHV-JHM infection was most evident in lamina 3 at both days 3 and 4 (Fig. 2C, D). Infected cells were seen throughout the depth of this lamina, although the labeling was less evenly dispersed than that seen with HSV-1. Virus was also detected in laminae 1 and 2, with infection of sublaminae 1a and 2b being most common. As with HSV-1, infection of the medial prefrontal cortex was common, particularly by day 4. Labeling in the medial and lateral orbital cortices was first detected in lamina 5, extending into laminae 2, 3 and 6 at day 4. Infection of the anterior cingulate cortex was also restricted to lamina 5 in several cases, with eventual spread to all laminae at day 4. Infralimbic cortex was infected in every case, virus first

appearing in lamina 6 (Fig. 1C), with spread to the other laminae, particularly lamina 5, in half of the cases.

More caudally, MHV-JHM infected the entorhinal and perirhinal cortices. Similar to the HSV-1 infection of entorhinal cortex, laminae 2, 3 and 5 were most commonly labeled, although laminae 1 and 6 were also infected in several mice. Infection of perirhinal cortex was seen in all cases at day 3, but was restricted to lamina 6 only. By day 4, virus was detected in more superficial laminae in half of the cases. Infection of agranular insular cortex by MHV-JHM was seen in all cases at day 4, most commonly in lamina 5, but also in laminae 2, 3 and 6 in more extensively infected cases.

Basal forebrain. MHV-JHM infected the vertical and horizontal nuclei of the diagonal band and the medial septal nucleus in all mice by day 3 (Fig. 4A, B). The infection sometimes appeared to involve the entire extent of these nuclei, forming a continuous group of infected cells among these three structures. HSV-1, however, regularly infected the horizontal nucleus of the diagonal band, but not the vertical nucleus. Scattered HSV-1-infected cells were seen in the medial septal nucleus in half of the cases at day 5. By day 4, MHV-JHM had spread to other septal nuclei, including the lateral, triangular and septofimbrial nuclei. The lateral septal nucleus was also commonly infected by HSV-1.

Although both viruses infected the ventral pallidum, MHV-JHM infected this structure both earlier in the infection and more intensely. Labeled cells were evident from the rostral ventral pallidum to the most

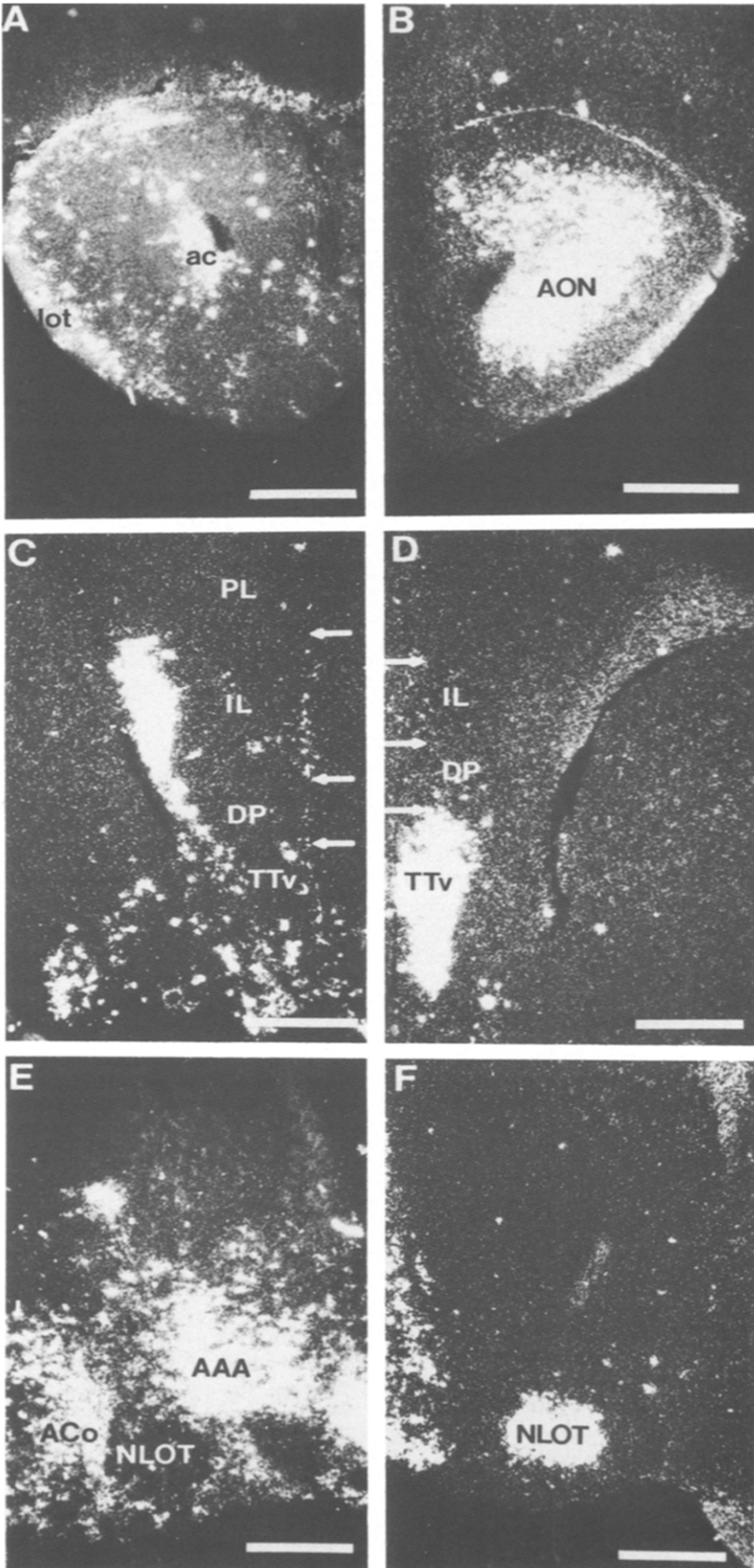


Fig. 1

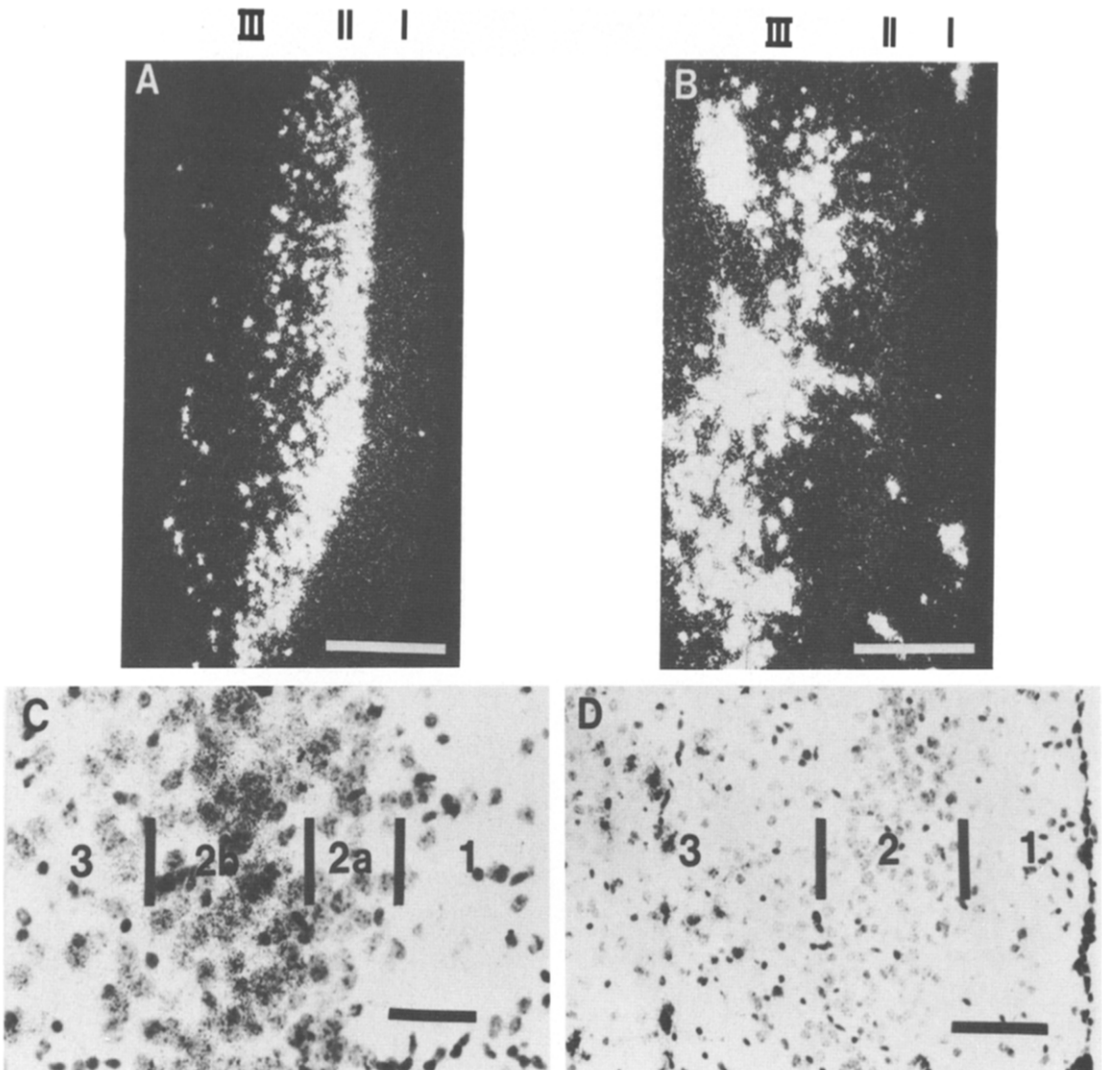


Fig. 2. HSV-1 and MHV-JHM differentially infect the laminae of the primary olfactory cortex. (A, C) HSV-1 infection of laminae 2b and 3 at day 4 p.i. (B, D) MHV-JHM infection of lamina 3 at day 3 p.i. Scale bars = 200 μm (A, B); 100 μm (C); 50 μm (D).

caudal aspect of this structure, where MHV-JHM also infected the ventral substantia innominata. MHV-JHM-infected cells were seen in the white matter of the anterior commissure (Fig. 1A) in all mice. Overall, MHV-JHM infection of the basal forebrain was more widespread than that with HSV-1.

Amygdala. Both viruses consistently infected the anterior and medial cortical amygdaloid nuclei, while

MHV-JHM infected the anterior amygdaloid area more commonly (Fig. 1E). With the exception of these structures, infection of the amygdala was more prominent with HSV-1. The posterior medial and posterior lateral nuclei were more commonly infected by HSV-1 (Fig. 3C, D), with labeling in both of these structures in all day 5 cases. HSV-1 labeling was detected throughout the rest of the amygdala, including the basolateral, basomedial and central nuclei.

Fig. 1. Dark-field photomicrographs of primary MOB connections which are infected differentially by MHV-JHM (A, C, E) and HSV-1 (B, D, F) following intrabulbar inoculation. (A) MHV-JHM infection of the anterior olfactory nucleus, anterior commissure (ac) and the lateral olfactory tract (lot). (B) HSV-1 infection of the anterior olfactory nucleus (AON). (C) MHV-JHM infection of lamina 6 of the infralimbic cortex (IL), but not the ventral tenia tecta (TTv). (D) Intense infection of the ventral tenia tecta by HSV-1. (E) MHV-JHM infection of the anterior cortical amygdaloid nucleus (ACo) and the anterior amygdaloid area (AAA), without labeling over the nucleus of the lateral olfactory tract (NLOT). (F) HSV-1 infection of the nucleus of the lateral olfactory tract. DP, dorsal peduncular cortex; PL, prelimbic cortex. Scale bars = 500 μm .

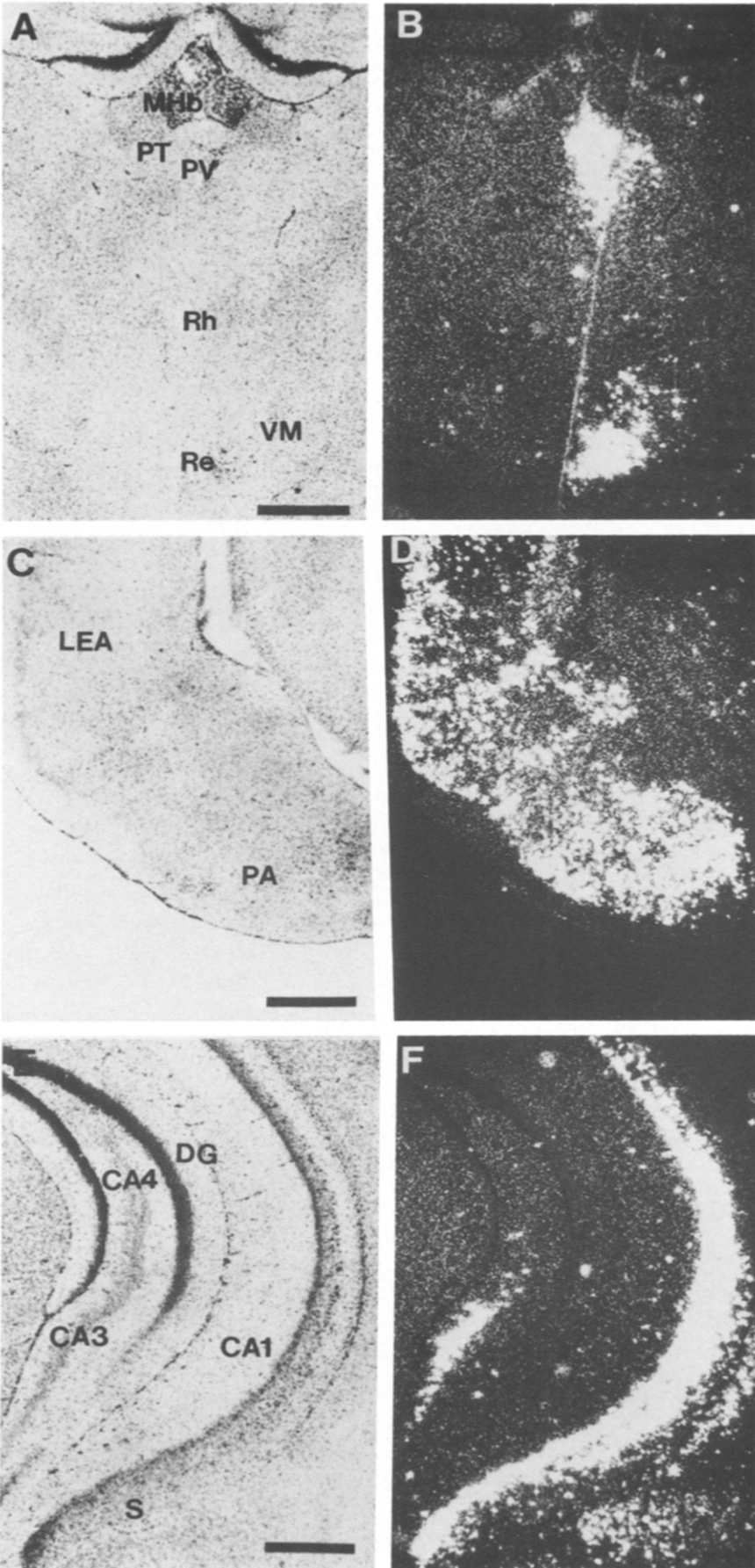


Fig. 3
1014

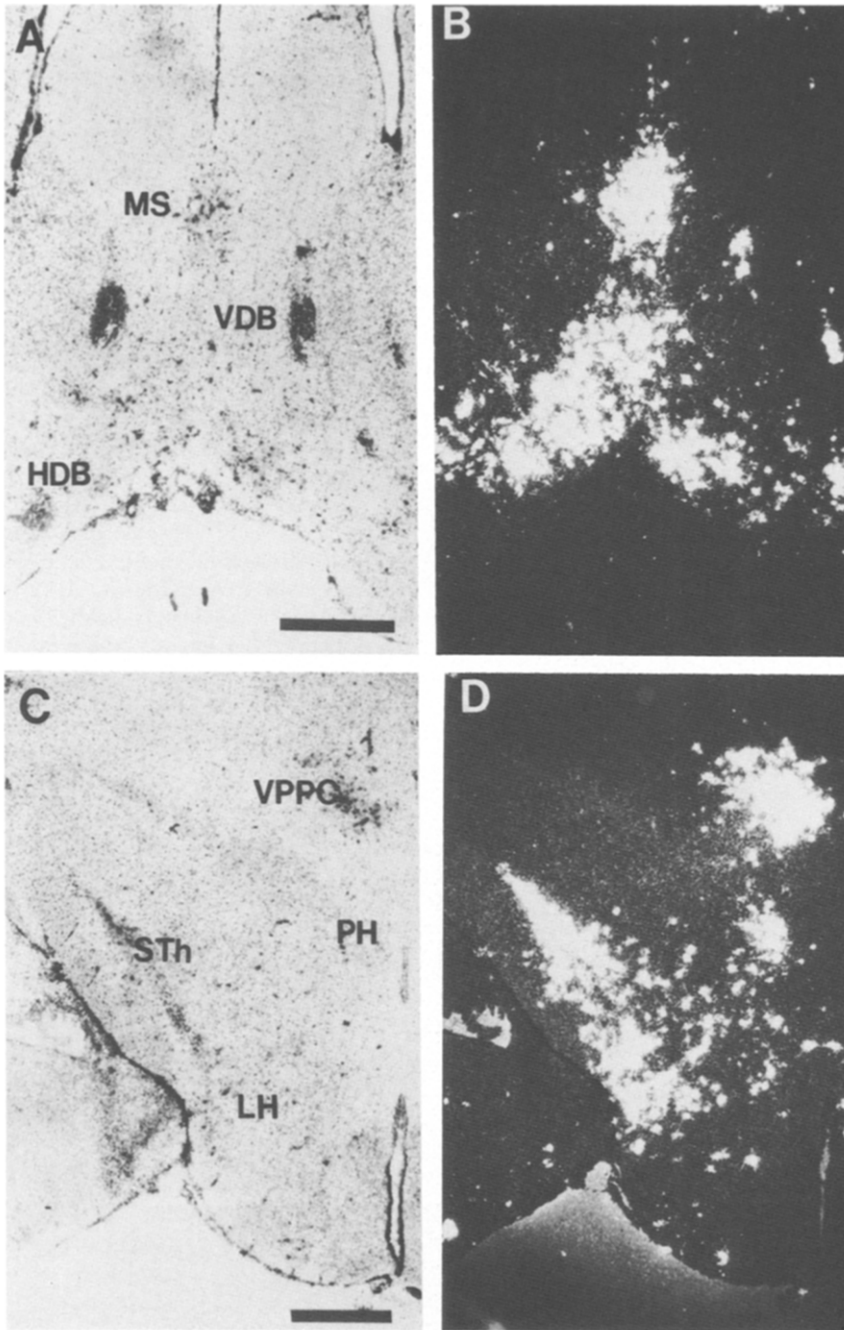


Fig. 4. Matching bright-field and dark-field photomicrographs of structures infected primarily by MHV-JHM. (A, B) Infection of the medial septal nucleus (MS), horizontal (HDB) and vertical (VDB) nuclei of the diagonal band. (C, D) Infection of the ventroposterior parvocellular thalamus (VPPC), posterior (PH) and lateral (LH) hypothalamic areas, and subthalamic nucleus (STh). Scale bars = 500 μ m.

Fig. 3. Matching bright-field and dark-field photomicrographs of structures infected primarily by HSV-1 following intralobar inoculation. (A, B) Infection of the reuniens (Re) and paraventricular (PV) thalamic nuclei. (C, D) Infection throughout the lateral entorhinal area (LEA) and the posterior amygdala (PA). (E, F) Labeling in the pyramidal cell layer of CA1 and CA3, the stratum oriens of CA1 and the subiculum (S). DG, dentate gyrus; MHb, medial habenular nucleus; PT, paratenial thalamic nucleus; Rh, rhomboid thalamic nucleus; VM, ventromedial thalamic nucleus. Scale bars = 500 μ m.

The nucleus of the lateral olfactory tract was also infected by HSV-1 in the majority of cases by day 5 (Fig. 1F).

Diencephalon. Thalamic infection by HSV-1 was primarily restricted to the midline nuclei, including the paratenial, paraventricular and reuniens nuclei (Fig. 3A, B). MHV-JHM labeling was detected less frequently in these structures. The ventroposterior parvocellular thalamus, however, was infected by MHV-JHM in all cases at day 4 (Fig. 4C, D). This structure was never infected by HSV-1, even at day 5.

In the hypothalamus, HSV-1 infected scattered cells in the lateral hypothalamus at day 5. MHV-JHM infected this area in almost every case at both days 3 and 4, although the labeling was commonly sparse. Strong labeling was commonly detected in the nearby subthalamic nucleus and the posterior hypothalamic area (Fig. 4C, D). The stria medullaris also contained cells infected by MHV-JHM.

Hippocampal complex. Hippocampal infection by HSV-1 was seen in every case at both four and five days. At day 4, CA1 pyramidal cells were infected in all four mice. By day 5, infection of the stratum oriens of CA1 and the pyramidal layer of CA3 occurred in half of the mice (Fig. 3E, F). Labeling was also

detected in the granule cell layer and less commonly in the polymorph layer of the dentate gyrus. In sharp contrast to this pattern of spread throughout the hippocampus, MHV-JHM sparsely infected only a small area of the CA1 region in one case at day 4. Infection of the indusium griseum by MHV-JHM was seen in all cases by day 4 and in almost half of the HSV-1-infected brains. MHV-JHM labeling in the indusium griseum continued caudally into the dorsal subicular portion of the hippocampal complex at the splenium of the corpus callosum. Infection of the subiculum by HSV-1 also occurred by day 5, although the ventral subiculum was more commonly involved (Fig. 3E, F).

Midbrain. MHV-JHM was detected in the ventral tegmental area (VTA) in all cases at day 3. The infection progressed to involve the entire structure at day 4, as well as the adjacent substantia nigra pars compacta. Labeling was noted in a caudal and dorsal direction throughout the tegmentum, continuous with that in the VTA. In contrast, HSV-1 infection of the VTA was not commonly detected until day 5 and was generally less intense. More caudally, HSV-1 infection of the caudal linear raphe nucleus was also seen at this time. Both the median and dorsal raphe

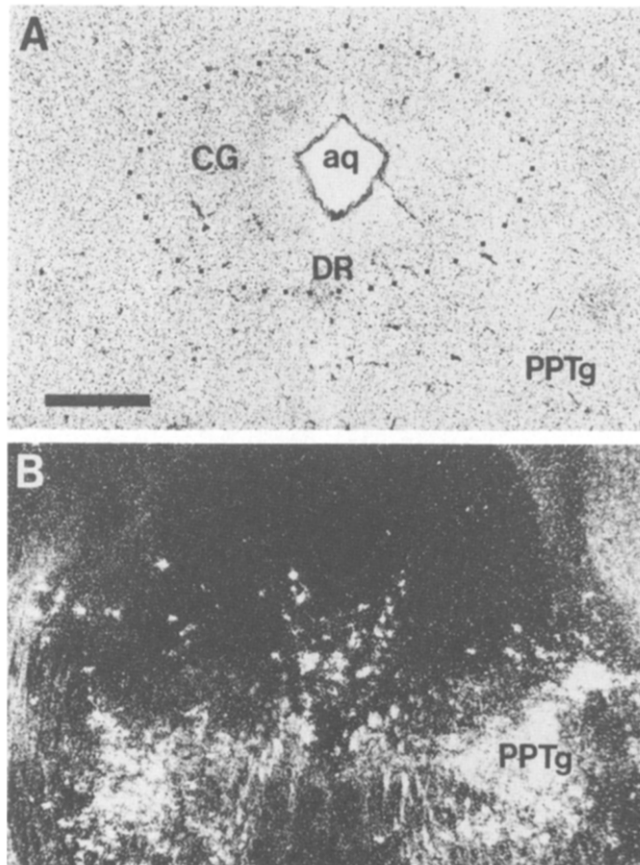


Fig. 5. MHV-JHM infection of the pedunculo-pontine tegmental nuclei (PPTg) lateral to the superior cerebellar peduncles, as well as in the dorsal raphe (DR). aq, cerebral aqueduct; CG, central gray. Scale bar = 500 μ m.

nuclei were infected by MHV-JHM and HSV-1 with equal frequency.

The propensity of MHV-JHM to infect cholinergic structures, as seen in the basal forebrain, continued as the pedunculopontine tegmental nucleus was infected in almost every case (Fig. 5A, B). This structure is continuous with the more caudal parabrachial complex, which was also commonly infected. Viral RNA was consistently located in the region of the medial parabrachial nucleus, which lies ventral to the superior cerebellar peduncle. HSV-1 did not infect these structures, but instead infected the nearby LC. HSV-1 infection was characterized by a dense infection of the full extent of the LC in every case. By day 5, labeling often continued caudally along the lateral borders of the fourth ventricle.

Pons and medulla. Infection of structures caudal to the LC in HSV-1-infected mice was not common, even at day 5 p.i. The main exceptions were infected cells in the area of the A1 and A2 groups, which were present in more extensively infected brains. Infection of brainstem raphe nuclei by HSV-1 occurred rarely, while the raphe magnus and raphe obscurus were infected by MHV-JHM in most cases. In addition, MHV-JHM regularly infected several parts of the brainstem reticular formation, including the oral

and caudal pontine reticular nuclei and the nucleus gigantocellularis.

Lateral ventricle inoculations

Inoculations into the lateral ventricle were performed to determine the possible contribution of cerebrospinal fluid spread to the observed distribution of virus. The pattern of infection seen following lateral ventricle inoculation with MHV-JHM at day 4 was quite distinct from that seen following intranasal and intrabulbar inoculation. Most of the structures infected were in close proximity to a ventricle, although not all juxtaventricular structures were labeled. Among the regions heavily infected were the septum, the bulk of the hypothalamus and the hippocampus. Detection of HSV-1 at day 5 following a lateral ventricle inoculation revealed a similar pattern. In both cases, several structures normally infected following intrabulbar inoculation, such as the primary olfactory cortex, showed little or no labeling.

Infection of dopaminergic and noradrenergic neurons

The VTA contains a dense collection of dopaminergic neurons which belong to the A10 group (Fig. 6A). Although relatively few cells in the VTA are infected by HSV-1 at 4.5 days p.i. (Fig. 6B),

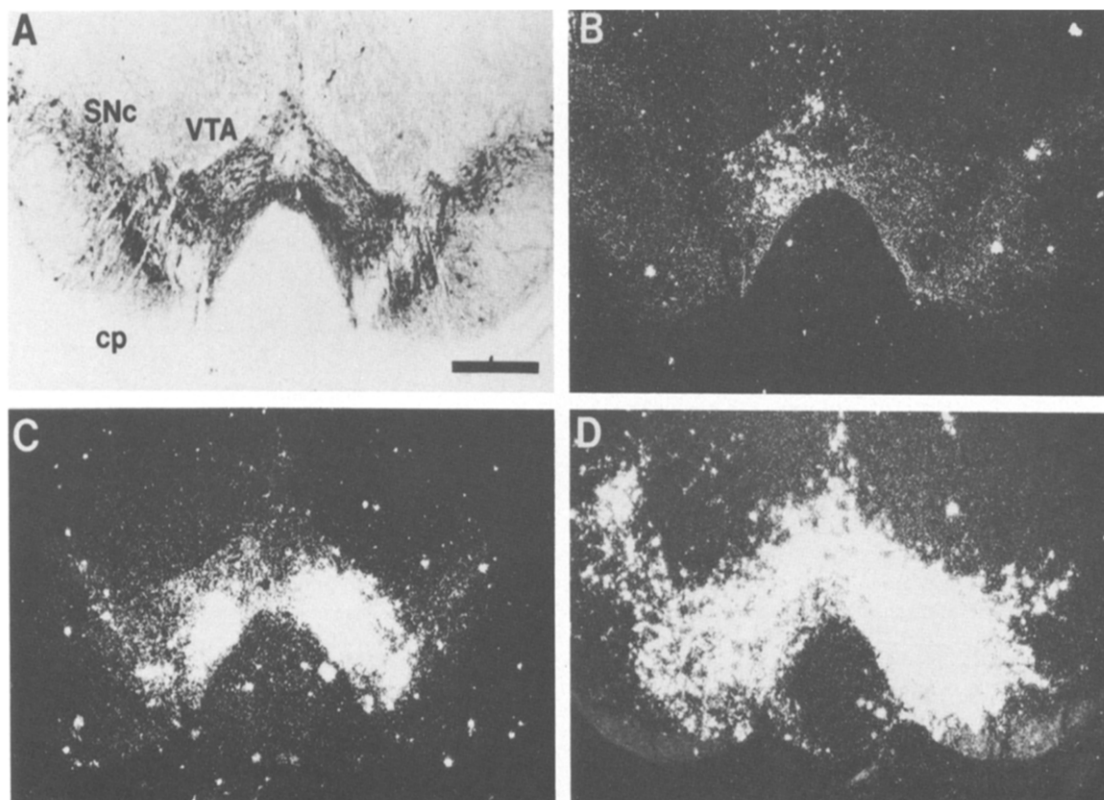


Fig. 6. Infection of the VTA by HSV-1 and MHV-JHM. (A) Immunohistochemistry for TH+ neurons of the VTA and substantia nigra pars compacta (SNc). (B) Dark-field photomicrograph of HSV-1 infection of this structure at 4.5 days p.i. (C, D) Corresponding sections showing infection of the VTA by MHV-JHM at days 3 (C) and 4 (D) p.i. Note infection of the substantia nigra pars compacta at day 4. cp, cerebral peduncle. Scale bar = 500 μ m.

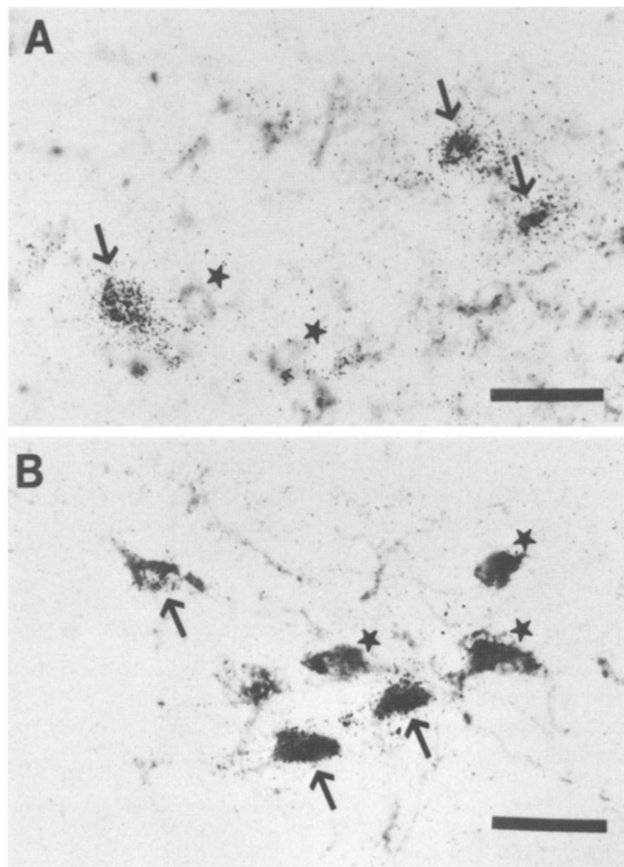


Fig. 7. HSV-1- and MHV-JHM-infected TH-immunoreactive cells. (A) Cells labeled for TH and MHV-JHM (arrows) and TH only (stars) in the VTA. (B) HSV-1-infected (arrows) and non-infected (stars) TH-immunoreactive neurons in the rostral LC. Scale bars = 5 μ m.

combined TH immunohistochemistry and *in situ* hybridization for viral nucleic acids revealed that the vast majority of HSV-1 infected cells in the VTA were also TH immunoreactive (TH+). MHV-JHM had already infected a larger number of cells in the VTA at day 3 (Fig. 6C) and the vast majority of infected cells were TH+ (Fig. 7A). By day 4, the full extent of the VTA was normally infected by MHV-JHM (Fig. 6D), although a smaller percentage of infected cells were also TH+. Additionally, MHV-JHM-infected TH+ cells were detected in the substantia nigra pars compacta (A9) and throughout the A8 dopaminergic group on day 4. The percentage of MHV-JHM-infected cells which were also TH+ appeared to decrease significantly as the number of infected cells in these structures increased.

Double labeling for TH and viral nucleic acid showed that HSV-1 infected the entire LC (A6), as dense silver grains were seen over TH+ cells in this structure (Fig. 8A, B). In sections where a relatively small number of cells in the LC were infected, the infection was restricted almost entirely to neurons which were TH+ (Fig. 7B). In sections where the infection of this structure was more widespread, the number of TH-immunonegative (TH-) cells infected

by HSV-1 increased dramatically. Although MHV-JHM infected a rare TH+ neuron in the dorsal LC, the vast majority of infected cells were clearly in the medial parabrachial nucleus (Fig. 8C, D).

DISCUSSION

This is the first study to show by direct comparison using identical experimental protocols that two different neurotropic viruses move along different neural pathways following inoculation into a common site. Our results indicate that MHV-JHM and HSV-1 spread along both common and unique pathways following intranasal and intrabulbar inoculations and that both viruses spread in a circuit-specific manner, since adjacent structures were infected by one virus or the other without contiguous (lateral) spread.

Methodological considerations

The present findings are broadly consistent with earlier studies examining the spread of HSV-1 and MHV after inoculation into the olfactory system^{40,47,55}. Although both viruses can spread via the cerebrospinal fluid, the pattern of infection following intraventricular inoculation suggests that virus

spread via the cerebrospinal fluid following intranasal and intrabulbar inoculations was minimal at the times p.i. examined in this study.

Many structures were infected on both the ipsilateral and contralateral sides at early times p.i., despite unilateral inoculation of virus. Infection of the anterior olfactory nuclei, which project to both the ipsilateral and contralateral MOB⁶³ was commonly bilateral for both viruses early in the infection. Virus can also spread to the contralateral side across commissural connections between the olfactory cortices. Contralateral primary olfactory cortex infection in HSV-1-infected brains was first seen in lamina 2b, from which commissural projections arise.²⁴ MHV-JHM was detected in cells in the anterior commissure, through which these commissural projections cross. This is consistent with similar labeling in mice infected intranasally following unilateral bullectomy.⁵⁶ Intranasal inoculation in that study quickly resulted in a bilateral infection also, despite the fact that MHV-JHM entry was restricted to the side with an intact MOB.

Some of the labeling in heavily infected structures was likely related to infection of glia, and both MHV-JHM and HSV-1 have been shown to infect

glia during CNS infections.^{5,33,47,52} Consistent with this, the percentage of TH⁺ cells in the LC infected with HSV-1 and in the A8–A10 groups infected with MHV-JHM increased as the infections intensified. Reactive gliosis, during which glia form a barrier around lysed neurons, may actually prevent the non-specific spread of virions in the extracellular space, thereby contributing to the specificity of trans-neuronal movement of virus.⁵⁸

Comparative anatomy of MHV-JHM and HSV-1 infections

Primary olfactory connections. Both viruses infected the majority of the primary connections of the MOB, as revealed by conventional tracing studies done in rodents.^{11,45,63,73} The early infection of MOB afferents which do not receive a reciprocal projection from the bulb, such as the horizontal nucleus of the diagonal band, is consistent with retrograde movement of these two viruses within the CNS. The relatively light infection of the olfactory tubercle by both viruses suggests a slowness/absence of anterograde movement, as this structure receives a non-reciprocal afferent from the MOB. On the other hand, anterograde virus spread occurred from the olfactory

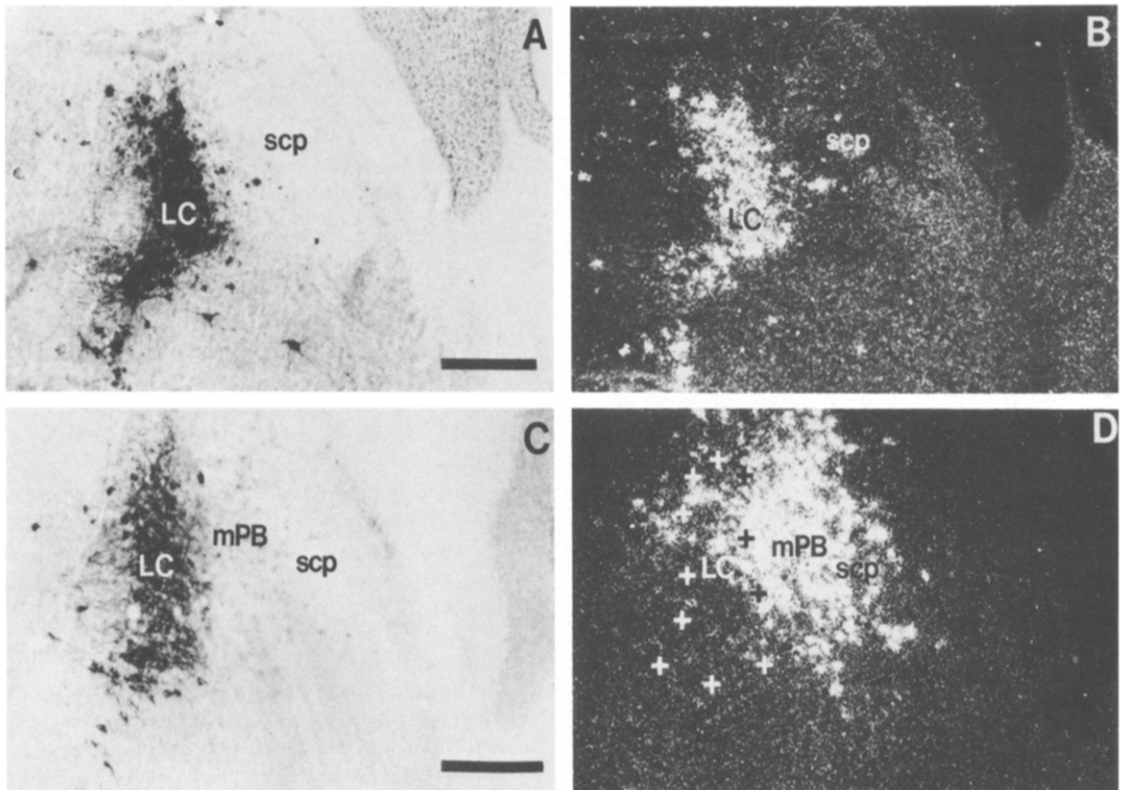


Fig. 8. Immunohistochemistry for TH combined with *in situ* hybridization for HSV-1 (A, B) or MHV-JHM (C, D). Corresponding bright-field and dark-field photomicrographs of the region of the locus coeruleus and the parabrachial complex. (A, C) TH immunoreactivity of A6 noradrenergic neurons in the LC. (B) HSV-1 infection is restricted to the noradrenergic neurons of the LC. (D) MHV-JHM infects the adjacent medial parabrachial nucleus (mPB), between the LC and the superior cerebellar peduncle (scp).

The location of the LC is denoted by the crosses. Scale bars = 300 μ m.

anterior olfactory nuclei, entorhinal cortex and the CA1 region of Ammon's horn.²⁷ The subthalamic nucleus, which projects to both the ventral pallidum and the lateral hypothalamus,^{22,32} was infected exclusively by MHV-JHM.

HSV-1 regularly infected several regions of the hippocampus, a structure infected only rarely by MHV-JHM. In addition to the previously mentioned infection of CA1, CA3 pyramidal cells and granule cells of the dentate gyrus were also infected by HSV-1. The pattern of viral spread within the hippocampus was suggestive of retrograde transport. HSV-1 was detected in CA3 only in cases when the CA1 region, to which it projects,⁷² was also infected. Similarly, the granule cells of the dentate gyrus were only infected following CA3 infection, consistent with retrograde spread from the CA3 region, to which it projects.⁴¹

Whereas HSV-1 infected the LC, MHV-JHM infected the pedunculo-pontine tegmental nucleus and the medial parabrachial nucleus. The latter two structures are continuous and together extend along the full rostral-caudal extent of the LC. The pedunculo-pontine tegmental nucleus projects to several structures infected exclusively or more prominently by MHV-JHM, including the VTA, subthalamic nucleus and the lateral hypothalamus.^{31,60,69} The medial parabrachial nucleus projects to a number of MHV-JHM-infected structures, including insular cortex, the lateral hypothalamus and the ventroposterior parvocellular thalamus.^{19,50,59,66}

In the cortex, both viruses commonly infected laminae 2, 3 and 5 of entorhinal cortex, consistent with a projection from laminae 2 and 3 to the MOB⁶³ and projections from the deep layers of the entorhinal cortex to primary olfactory cortex.⁷¹ Laminae 2, 5 and 6 of agranular insular cortex were also infected by both viruses. Cells in lamina 5 of this cortical area project to the lateral hypothalamic area, while those in all three laminae project to infralimbic cortex.¹ Commonly, cortical infections were first restricted to specific lamina or laminae, with eventual involvement of additional laminae. In several cortical regions viral labeling was eventually seen in every lamina, suggesting intracortical spread of virus.

Differential infection of dopaminergic and noradrenergic neurons

Both viruses were shown to infect cells in the VTA, which contains a dense collection of dopaminergic neurons belonging to the A10 group. The VTA-substantia nigra projects to a number of structures, including primary olfactory cortex, the nuclei of the diagonal band, and the medial prefrontal, insular and entorhinal cortices.^{4,42,70} MHV-JHM infected this area more intensely and earlier in the course of the infection than HSV-1, and also infected dopaminergic neurons in the A8 and A9 groups. Both viruses primarily infected TH+ neurons early in their infection of the VTA. By day 4, only about one-half

of the MHV-JHM-infected cells were TH+ in this region. One possible explanation for this finding is that MHV-JHM infects both dopaminergic and non-dopaminergic neurons in this structure, since one-third of VTA neurons are non-dopaminergic and many projections arise from both dopaminergic and non-dopaminergic neurons.⁷⁰ Another explanation is an increase in the infection of glial cells following virus spread from adjacent infected neurons.

Combined assay for virus and TH clearly showed that HSV-1 infected noradrenergic neurons in the LC, whereas MHV-JHM did not. This finding suggests that either MHV-JHM lacks the ability to infect noradrenergic fibers arising from the LC or, alternatively, that the virus does not cross the appropriate synapses to gain access to LC terminals. Recent studies indicate that, in the rat, the noradrenergic input from the LC terminates in the internal and external plexiform layers and granule cell layer in the MOB, but not in the glomerular layer.⁴⁸ The granule cells of the MOB form dendrodendritic contacts with mitral and tufted cells,⁶² which provide efferent fibers of the MOB. A failure of MHV-JHM to enter the granule cells via the dendrodendritic contacts with the mitral and tufted cells would prevent access to the noradrenergic input from the LC. Inability of MHV-JHM to infect LC neurons appears more likely since MHV-JHM infection of the internal granular layer of the MOB was seen following intranasal inoculation. In addition, direct MOB inoculations of MHV-JHM, which would be expected to expose LC terminals to virus, did not result in infection of this structure. Finally, the LC projects to a number of other structures infected by MHV-JHM (e.g. anterior olfactory nuclei, primary olfactory cortex, the VTA, entorhinal cortex), but was still not infected.

Determinants of specific viral spread

There are a number of possible explanations for the differences described above between MHV-JHM and HSV-1 spread. The steps involved in the transneuronal spread of virus include, but are not restricted to, axonal transport of virus, viral exit from the presynaptic cell and uptake at the postsynaptic cell. Differences between viruses at any of these steps would result in unique patterns of viral spread.

Although anterograde axonal transport and anterograde movement across the synapse are both probably involved in the spread of virus from the olfactory epithelium to the brain, anterograde spread once inside the brain is relatively inefficient. The direction of HSV-1 transneuronal movement is strain dependent,⁸⁴ but our results suggest that HSV-1 strain 17 utilizes retrograde axonal transport and transneuronal movement once inside the brain. Since both HSV-1 and MHV-JHM show preferential retrograde transport, this does not explain the observed differences between them.

Viral exit from the cell may occur preferentially at a particular site (e.g. dendrites vs soma), exposing only neurons synapsing in that location to virus. HSV-1, a DNA virus which replicates in the nucleus, buds from the nuclear membrane. MHV, an RNA virus, replicates in the cytoplasm, budding into transitional vesicles between the rough endoplasmic reticulum and Golgi apparatus,⁷⁶ which are then segregated into the constitutive exocytic pathway.⁷⁷ While the relationship between virus budding and exit from specific sites in the cell has not been established for either MHV or HSV-1, this could contribute to the pattern of virus spread.

Since both MHV-JHM and HSV-1 are believed to enter susceptible cells by a receptor-mediated process, the observed patterns of spread may result from the presence of a virus receptor on the postsynaptic neuron. The inability of MHV-JHM to infect the LC, as discussed above, may reflect the absence of the MHV receptor on these neurons. In addition, the cellular location of the receptor on neurons might determine whether anterograde transneuronal movement occurs. If the receptor is located only on the axon terminal, anterograde movement at an axodendritic or dendrodendritic synapse would be unlikely.

The receptor for MHV has been identified as one or more members of the murine carcinoembryonic antigen family of glycoproteins.^{14,81-83} Although the CNS receptor for HSV-1 has not been fully characterized, at least two HSV-1 receptors which bind different viral glycoproteins are expressed on some cells,⁶¹ possibly providing the basis by which strains which differ in surface glycoprotein expression can differ in the direction of transneuronal movement. As more is known regarding the distribution of the cellular receptors for these two viruses, it will be possible to correlate the pattern of viral spread with the distribution of the receptor.

Finally, viruses may differ in uptake between neurons of different neurotransmitter systems. In addition to its inability to infect the LC, MHV-JHM did not infect other noradrenergic cells groups in the brainstem, despite infection of a large number of brainstem structures. In contrast, both viruses infected the dopaminergic neurons of the VTA. It is possible that the inability of MHV-JHM to infect noradrenergic neurons in part determined the pattern of spread observed. Further studies are underway to determine the relative importance of this factor in viral spread.

Implications for viral tracing and neurological disease

Viruses that spread transneuronally have become increasingly popular as neural tracers.³⁷ Pseudorabies virus has been used primarily as a tracer for mapping out central connections of peripheral nerves and typically crosses two to three synapses.^{7,68} Both MHV and HSV-1 are useful as systems tracers after direct inoculation into the brain, since they can cross several synapses in a circuit-specific manner. A common assumption underlying the use of viruses for neural

tracing is that they move non-specifically along all the available neural pathways, infecting all of the neurons which synapse on infected neurons. Our results show quite clearly, however, that MHV-JHM and HSV-1 infect only a subset of MOB connections. The spread of these viruses along unique routes following a common inoculation site indicates that they may be most useful for identifying distinct transneuronal pathways from a structure.

Our results also have implication for the pathogenesis of neurological diseases, such as Alzheimer's disease and Parkinson's disease, which may result from virus destruction of neurons or may be triggered by a prior viral infection.^{15,20} Pathways exist from the MOB to a number of CNS structures affected in various neurological diseases, including, most notably, Alzheimer's disease.^{30,57} Our results indicate that it is possible for a virus to enter the MOB and infect only a subset of connected structures. In addition, our results also show that two different viruses could enter the CNS via the olfactory epithelium (or possibly another entry site) and spread to infect different subsets of connected structures. The resulting clinical and pathological manifestations would be very different, even though the site of entry and spread via a transneuronal route would be the same. Further studies using other strains of HSV-1 or MHV, or other neurotropic viruses, may provide additional evidence for an infectious component to some neurological diseases.

CONCLUSIONS

Both HSV-1 and MHV-JHM spread transneuronally, in a circuit-specific manner, after intranasal or intrabulbar inoculation. Most significantly, while both viruses infected many of the same MOB connections, a number of structures were infected exclusively by one of the two viruses. We conclude from these observations that each virus infects a distinct, but partially overlapping, set of neural pathways originating from the MOB. Some of this specificity appears to be determined by differential infection of neurons expressing specific neurotransmitters, although differences in access to synapses and in receptor distributions most likely also contribute to the observed patterns of infection. This specificity suggests that different viruses will be useful for analysing different neural circuits originating from a structure. Lastly, these two neurotropic viruses entered the CNS through a natural route of entry and localized to specific structures, showing that, despite a common site of entry, different viruses may cause neurological disease involving different regions of the brain.

Acknowledgements—We thank Drs M. Brown and Ed Wagner for providing HSV-1, strain 17 and a plasmid containing the VP-5 gene of HSV-1, respectively. We thank Gregory Evans for helpful discussions and Paul Reimann

for excellent photographic assistance. This work was supported by grants from N.I.H. (NS24401 and DC01711) and from the National Multiple Sclerosis Society. S.P. was supported by a N.I.H. Research Career Development Award and E.M.B. by an NIMH Predoctoral M.D./Ph.D. Fellowship (MH10384).

REFERENCES

- Allen G. V., Saper C. B., Hurley K. M. and Cechetto D. F. (1991) Organization of visceral and limbic connections in the insular cortex of the rat. *J. comp. Neurol.* **311**, 1–16.
- Barnett E. M. and Perlman S. (1993) The olfactory nerve and not the trigeminal nerve is the main route of entry for mouse hepatitis virus strain JHM. *Virology* (in press).
- Barthold S. W. (1988) Olfactory neural pathways in mouse hepatitis virus nasooencephalitis. *Acta neuropath.* **76**, 502–506.
- Beckstead R. M., Domesick V. B. and Nauta W. J. H. (1979) Efferent connections of the substantia nigra and ventral tegmental area in the rat. *Brain Res.* **175**, 191–217.
- Blessing W. W., Li Y.-W. and Wesselingh S. L. (1991) Transneuronal transport of herpes simplex virus from the cervical vagus to brain neurons with axonal inputs to central vagal sensory nuclei in the rat. *Neuroscience* **42**, 261–274.
- Buchmeier M. J., Lewicki H. A., Talbot P. J. and Knobler R. L. (1984) Murine hepatitis virus-4 (strain JHM)-induced neurological disease is modulated *in vivo* by monoclonal antibody. *Virology* **132**, 261–270.
- Card J. P., Rinaman L., Schwaber J. S., Miselis R. R., Whealy M. E., Robbins A. K. and Enquist L. W. (1990) Neurotropic properties of pseudorabies virus: uptake and transneuronal passage in the rat central nervous system. *J. Neurosci.* **10**, 1974–1994.
- Card J. P., Whealy M. E., Robbins A. K., Moore R. Y. and Enquist L. W. (1991) Two alpha-herpes virus strains are transported differentially in the rodent visual system. *Neuron* **6**, 957–969.
- Cheever F. S., Daniels J. B., Pappenheimer A. M. and Bailey O. T. (1949) A murine virus (JHM) causing disseminated encephalomyelitis with extensive destruction of myelin. *J. exp. Med.* **90**, 181–194.
- Dalziel R. G., Lampert P. W., Talbot P. J. and Buchmeier M. J. (1986) Site-specific alteration of murine hepatitis virus type 4 peplomer glycoprotein E2 results in reduced neurovirulence. *Virology* **59**, 461–471.
- de Olmos J., Hardy H. and Heimer L. (1978) The afferent connections of the main and the accessory olfactory bulb formations in the rat: an experimental HRP-study. *J. comp. Neurol.* **181**, 213–244.
- de Olmos J., Alheid G. F. and Beltramino C. A. (1985) Amygdala. In *The Rat Nervous System* (ed. Paxinos G.), Vol. 1, pp. 223–334. Academic Press, New York.
- Dix R. D., McKendall R. R. and Baringer J. R. (1983) Comparative neurovirulence of herpes simplex virus type 1 strains after peripheral or intracerebral inoculation of BALB/C mice. *Infect. Immun.* **40**, 103–112.
- Dveksler G. S., Pensiero M. N., Cardellichio C. B., Williams R. K., Jiang G.-S., Holmes K. V. and Dieffenbach C. W. (1991) Cloning of the mouse hepatitis virus (MHV) receptor: expression in human and hamster cell lines confers susceptibility to MHV. *J. Virol.* **65**, 6881–6891.
- Elizan T. S. and Casals J. (1991) Astrogliosis in von Economo's and postencephalitis Parkinson's diseases supports probable viral etiology. *J. neuropath. Sci.* **105**, 131–134.
- Fallon J. H. and Moore R. Y. (1978) Catecholamine innervation of basal forebrain: III. Olfactory bulb, anterior olfactory nuclei, olfactory tubercle and piriform cortex. *J. comp. Neurol.* **189**, 533–544.
- Finger T. E. and Bottger B. (1991) Trigeminal sensory axons provide peptidergic innervation to glomeruli of the olfactory bulb. *Soc. Neurosci. Abstr.* **17**, 146.
- Fleming J. O., Trousdale M. D., El-Zaatari F. A. K., Stohlman S. A. and Weiner L. P. (1986) Pathogenicity of antigenic variants of murine coronavirus JHM selected with monoclonal antibodies. *Virology* **58**, 869–875.
- Fulwiler C. E. and Saper C. B. (1984) Subnuclear organization of the efferent connections of the parabrachial nucleus in the rat. *Brain Res.* **7**, 229–259.
- Gautrin D. and Gauthier S. (1989) Alzheimer's disease: environmental factors and etiologic hypotheses. *Can. J. neuropath. Sci.* **16**, 375–387.
- Goto N., Hirano N., Aiuchi M., Hayashi T. and Fujiwara K. (1977) Nasooencephalopathy of mice infected intranasally with a mouse hepatitis virus, JHM strain. *Jap. J. exp. Med.* **47**, 59–70.
- Groenewegen H. J. and Berendse H. W. (1990) Connections of the subthalamic nucleus with ventral striatopallidal parts of the basal ganglia in the rat. *J. comp. Neurol.* **294**, 607–622.
- Grove E. A. (1988) Efferent connections of the substantia innominata in the rat. *J. comp. Neurol.* **277**, 347–364.
- Haberly L. B. and Price J. L. (1978) Association and commissural fiber systems of the olfactory cortex of the rat: I. Systems originating in the piriform cortex and adjacent areas. *J. comp. Neurol.* **178**, 711–740.
- Haberly L. B. and Price J. L. (1978) Association and commissural fiber systems of the olfactory cortex of the rat: II. Systems originating in the olfactory peduncle. *J. comp. Neurol.* **178**, 781–808.
- Haspel M. V., Lampert P. W. and Oldstone M. B. A. (1978) Temperature-sensitive mutants of mouse hepatitis virus produce a high incidence of demyelination. *Proc. natn. Acad. Sci. U.S.A.* **75**, 4033–4036.
- Herkenham M. (1978) The connections of the nucleus reuniens thalami: evidence for a direct thalamo-hippocampal pathway in the rat. *J. comp. Neurol.* **177**, 589–610.
- Hoover J. E. and Strick P. L. (1993) Multiple output channels in the basal ganglia. *Science* **259**, 819–821.
- Hudson S. J., Dix R. D. and Streilein J. W. (1991) Induction of encephalitis in SJL mice by intranasal infection with herpes simplex virus type 1: a possible model of herpes simplex encephalitis in humans. *J. inf. Dis.* **163**, 720–727.
- Hyman B. T., Arriagada P. V. and Van Hoesen G. W. (1991) Pathologic changes in the olfactory system in aging and Alzheimer's disease. *Ann. N. Y. Acad. Sci.* **640**, 14–19.
- Jackson A. and Crossman A. R. (1983) Nucleus tegmenti pedunculopontinus: efferent connections with special reference to the basal ganglia, studied in the rat by anterograde and retrograde transport of horseradish peroxidase. *Neuroscience* **10**, 725–765.
- Kita H. and Kitai S. T. (1987) Efferent projections of the subthalamic nucleus in the rat: light and electron microscopic analysis with the PHA-L method. *J. comp. Neurol.* **260**, 435–452.
- Knobler R. L., Dubois-Dalq M., Haspel M. V., Claysmith A. P., Lampert P. W. and Oldstone M. B. (1981) Selective localization of wild type and mutant mouse hepatitis virus (JHM strain) antigens in CNS tissue by fluorescence, light and electron microscopy. *J. Neuroimmun.* **1**, 81–92.

34. Kovacs F. and Mettenleiter T. C. (1991) Firefly luciferase as a marker for herpes virus (pseudorabies virus): replication *in vitro* and *in vivo*. *J. gen. Virol.* **72**, 2999–3008.
35. Kristensson D., Ghetti B. and Wisniewski H. M. (1974) Study on the propagation of herpes simplex virus (type 2) into the brain after intraocular injection. *Brain Res.* **69**, 189–201.
36. Kucera P., Dolivo M., Coulon P. and Flamand A. (1985) Pathways of the early propagation of virulent and avirulent rabies strains from the eye to the brain. *J. Virol.* **55**, 158–162.
37. Kuypers H. G. J. M. and Ugolini G. (1990) Viruses as transneuronal tracers. *Trends Neurosci.* **13**, 71–76.
38. Lafay F., Coulon P., Astic L., Saucier D., Riche D., Holley A. and Flamand A. (1991) Spread of the CVS strain of rabies virus and of the avirulent mutant AvO1 along the olfactory pathways of the mouse after intranasal inoculation. *Virology* **183**, 320–330.
39. Lampert P. W., Sims J. K. and Kniazef A. J. (1973) Mechanism of demyelination in JHM virus encephalomyelitis. *Acta neuropath.* **24**, 76–85.
40. Lavi E., Fishman P. S., Highkin M. K. and Weiss S. R. (1988) Limbic encephalitis after inhalation of a murine coronavirus. *Lab. Invest.* **58**, 31–36.
41. Lorente de No R. (1934) Studies on the structure of the cerebral cortex: II. Continuation of the study of the ammonic system. *J. Psychol. Neurol.* **46**, 113–177.
42. Loughlin S. E. and Fallon J. H. (1984) Substantia nigra and ventral tegmental area projections to cortex: topography and collateralization. *Neuroscience* **11**, 425–435.
43. Lundh B., Kristensson K. and Norrby E. (1987) Selective infections of olfactory and respiratory epithelium by vesicular stomatitis and sendai viruses. *Neuropath. appl. Neurobiol.* **13**, 111–122.
44. Lundh B., Love A., Kristensson K. and Norrby E. (1988) Non-lethal infection of aminergic reticular core neurons: age-dependent spread of its mutant vesicular stomatitis virus from the nose. *J. Neuropath. exp. Neurol.* **47**, 497–506.
45. Macrides F. and Davis B. J. (1983) The olfactory bulb. In *Chemical Neuroanatomy* (ed. Emson P. C.), pp. 391–426. Raven Press, New York.
46. McLean I. W. and Nakane P. K. (1974) Periodate–lysine–paraformaldehyde fixative: a new fixative for immunoelectron microscopy. *J. Histochem. Cytochem.* **22**, 1077–1083.
47. McLean J. H., Shipley M. T. and Bernstein D. I. (1989) Golgi-like transneuronal retrograde labelling with CNS injections of herpes simplex virus type 1. *Brain Res. Bull.* **22**, 867–881.
48. McLean J. H., Shipley M. T., Nickell W. T., Aston-Jones G. and Reyher C. K. H. (1989) Chemoanatomical organization of the noradrenergic input from locus coeruleus to the olfactory bulb of the adult rat. *J. comp. Neurol.* **285**, 339–349.
49. Mesulam M.-M. (1978) Tetramethylbenzidine for horseradish peroxidase neurohistochemistry: a non-carcinogenic blue reaction product with superior sensitivity for visualizing neural afferents and efferents. *J. Histochem. Cytochem.* **26**, 106–117.
50. Moga M. M., Herbert H., Hurley K. M., Yasui Y., Gray T. S. and Saper C. B. (1990) Organization of cortical, basal forebrain, and hypothalamic afferents to the parabrachial nucleus in the rat. *J. comp. Neurol.* **295**, 624–661.
51. Morales J. A., Herzog S., Kompter C., Frese K. and Rott R. (1988) Axonal transport of Borna disease virus along olfactory pathways in spontaneously and experimentally infected rats. *Med. Microbiol. Immun.* **177**, 51–68.
52. Perlman S. and Ries D. (1987) The astrocyte is a target cell in mice persistently infected with mouse hepatitis virus, strain JHM. *Microb. Pathog.* **3**, 309–314.
53. Perlman S., Schelper R., Bolger E. and Ries D. (1987) Late onset, symptomatic, demyelinating encephalomyelitis in mice infected with MHV-JHM in the presence of maternal antibody. *Microb. Pathog.* **2**, 185–194.
54. Perlman S., Jacobsen G. and Moore S. (1988) Regional localization of virus in the central nervous system of mice persistently infected with murine coronavirus JHM. *Virology* **166**, 328–338.
55. Perlman S., Jacobsen G. and Afifi A. (1989) Spread of neurotropic murine coronavirus into the CNS via the trigeminal and olfactory nerves. *Virology* **170**, 556–560.
56. Perlman S., Evans G. and Afifi A. (1990) Effect of olfactory bulb ablation on spread of a neurotropic coronavirus in the mouse brain. *J. exp. Med.* **172**, 1127–1132.
57. Price J. L., Davis P. B., Morris J. C. and White D. L. (1991) The distribution of tangles, plaques and related immunohistochemical markers in healthy aging and Alzheimer's disease. *Neurobiol. Aging* **12**, 295–312.
58. Rinaman L., Card J. P. and Enquist L. W. (1993) Spatiotemporal responses of astrocytes, ramified microglia, and brain macrophages to central neuronal infection with pseudorabies virus. *J. Neurosci.* **13**, 685–702.
59. Saper C. B. and Loewy A. D. (1980) Efferent connections of the parabrachial nucleus in the rat. *Brain Res.* **197**, 291–317.
60. Saper C. B. and Loewy A. D. (1982) Projections of the pedunculopontine tegmental nucleus in the rat: evidence for additional extrapyramidal circuitry. *Brain Res.* **252**, 367–372.
61. Sears A. E., McGwire B. S. and Roizman B. (1991) Infection of polarized MDCK cells with herpes simplex virus 1: two asymmetrically distributed cell receptors interact with different viral proteins. *Proc. natn. Acad. Sci. U.S.A.* **88**, 5087–5091.
62. Shepherd G. M. (1972) Synaptic organization of the mammalian olfactory bulb. *Physiol. Rev.* **52**, 864–917.
63. Shipley M. T. and Adamek G. D. (1984) The connections of the mouse olfactory bulb: a study using orthograde and retrograde transport of wheat germ agglutinin conjugated to horseradish peroxidase. *Brain Res. Bull.* **12**, 669–688.
64. Shipley M. T. and Geinisman Y. (1984) Anatomical evidence for convergence of olfactory, gustatory, and visceral afferent pathways in mouse cerebral cortex. *Brain Res. Bull.* **12**, 221–226.
65. Shipley M. T., Halloran F. J. and de la Torre J. (1985) Surprisingly rich projection from locus coeruleus to the olfactory bulb in the rat. *Brain Res.* **329**, 294–299.
66. Shipley M. T. and Sander M. S. (1982) Special senses are really special: evidence for a reciprocal, bilateral pathway between insular cortex and nucleus parabrachialis. *Brain Res. Bull.* **8**, 493–501.
67. Slotnick B. M. and Leonard C. M. (1975) *A Stereotaxic Atlas of the Albino Mouse Forebrain*. Alcohol, Drug Abuse, and Mental Health Administration, Rockville, MD.
68. Strack A. M. and Loewy A. D. (1990) Pseudorabies virus: a highly specific transneuronal cell body marker in the sympathetic nervous system. *J. Neurosci.* **10**, 2139–2147.
69. Sugimoto T. and Hattori T. (1984) Organization and efferent projections of nucleus tegmenti pedunculopontinus pars compacta with special reference to its cholinergic aspects. *Neuroscience* **11**, 931–946.

70. Swanson L. W. (1982) The projections of the ventral tegmental area and adjacent regions: a combined fluorescent retrograde tracer and immunofluorescence study in the rat. *Brain Res. Bull.* **9**, 321–353.
71. Swanson L. W. and Kohler C. (1986) Anatomical evidence for direct projections from the entorhinal area to the entire cortical mantle in the rat. *J. Neurosci.* **6**, 3010–3023.
72. Swanson L. W., Sawchenko P. E. and Cowan W. M. (1981) Evidence for collateral projections by neurons in Ammon's horn, the dentate gyrus, and the subiculum: a multiple retrograde labeling study in the rat. *J. Neurosci.* **5**, 548–559.
73. Switzer R. C., de Olmos J. and Heimer L. (1985) Olfactory system. In *The Rat Nervous System* (ed. Paxinos G.), Vol. 1, pp. 1–36. Academic Press, New York.
74. Thomander L., Aldskogius H., Kristensson K., Vahlne A. and Thomas E. (1988) Invasion of cranial nerves and brain stem by herpes simplex virus inoculated into the mouse tongue. *Ann. Otol. Rhinol. Lar.* **97**, 554–558.
75. Tomlinson A. H. and Esiri M. M. (1983) Herpes simplex encephalitis: immunohistochemical demonstration of spread of virus via olfactory pathways in mice. *J. neuropath. Sci.* **60**, 473–484.
76. Tooze J., Tooze S. and Warren G. (1984) Replication of coronavirus MHV-A59 in sac- cells: determination of the first site of budding of progeny virions. *Eur. J. Cell Biol.* **33**, 281–293.
77. Tooze J., Tooze S. A. and Fuller S. D. (1987) Sorting of progeny coronavirus from condensed secretory proteins at the exit from the trans-Golgi network of AtT20 cells. *J. Cell Biol.* **105**, 1215–1226.
78. Van Groen T. and Wyss J. M. (1990) Extrinsic projections from area CA1 of the rat hippocampus: olfactory, cortical, subcortical, and bilateral hippocampal formation projections. *J. comp. Neurol.* **302**, 515–528.
79. Watts A. G. and Swanson L. W. (1989) Combination of *in situ* hybridization with immunohistochemistry and retrograde tract-tracing. In *Methods in Neuroscience* (ed. Conn P. M.), Vol. 1, pp. 127–135. Academic Press, New York.
80. Weiner L. P. (1973) Pathogenesis of demyelination induced by a mouse hepatitis virus. *Archs Neurol.* **28**, 298–303.
81. Williams R. K., Jiang G., Snyder S. W., Frana M. F. and Holmes K. V. (1990) Purification of the 110-kilodalton glycoprotein receptor for mouse hepatitis virus (MHV)-A59 from mouse liver and identification of a nonfunctional, homologous protein in MHV-resistant SJL/J mice. *J. Virol.* **64**, 3817–3823.
82. Williams R. K., Jiang G. and Holmes K. V. (1991) Receptor for mouse hepatitis virus is a member of the carcinoembryonic antigen family of glycoproteins. *Proc. natn. Acad. Sci. U.S.A.* **88**, 5533–5536.
83. Yokomori K. and Lai M. M. C. (1992) Mouse hepatitis virus utilized two carcinoembryonic antigens as alternative receptors. *J. Virol.* **66**, 6194–6199.
84. Zemanick M. C., Strick P. L. and Dix R. D. (1991) Direction of transneuronal transport of herpes simplex virus 1 in the primate motor system is strain-dependent. *Proc. natn. Acad. Sci. U.S.A.* **88**, 8048–8051.

(Accepted 18 June 1993)